3-11-2013

Microfluidic refractive index sensor based on an all-silica in-line Fabry–Perot interferometer fabricated with microstructured fibers

Jiajun Tian
University of Nebraska-Lincoln

Yujie Lu
University of Nebraska-Lincoln

Qi Zhang
University of Nebraska-Lincoln

Ming Han
University of Nebraska-Lincoln, mhan@egr.msu.edu

Microfluidic refractive index sensor based on an all-silica in-line Fabry–Perot interferometer fabricated with microstructured fibers

Jiajun Tian, Yujie Lu, Qi Zhang, and Ming Han*

Department of Electrical Engineering, University of Nebraska–Lincoln, Lincoln, Nebraska 68588, USA
mhan3@unl.edu

Abstract: We report a microfluidic fiber-optic refractive index (RI) sensor based on an in-line Fabry-Perot (FP) interferometer, which is formed by a silica tube sandwiched by two microstructured fibers (MFs). The sensor reported here can be fabricated at low cost, possess a robust structure, and has microfluidic capability. The micro-sized holes in the MFs naturally function as microfluidic channels through which liquid samples can be efficiently and conveniently delivered into and out of the FP cavity by a pressure/vacuum pump system for high-performance RI measurement. Due to the microfluidic capability enabled by the MFs, only sub microliter sample is required. We also experimentally study and demonstrate the superior performances of the sensor in terms of high RI sensitivity, good measurement repeatability, and low temperature cross-sensitivity.

OCIS codes: (060.2370) Fiber optics sensors; (120.3180) Interferometry; (120.2230) Fabry-Perot.

References and links

1. W. Liang, Y. Y. Huang, Y. Xu, R. K. Lee, and A. Yariv, "Highly sensitive fiber Bragg grating refractive index sensors," Appl. Phys. Lett. **86**(15), 151122 (2005).
2. I. Del Villar, I. R. Matias, and F. J. Arregui, "Enhancement of sensitivity in long-period fiber gratings with deposition of low-refractive-index materials," Opt. Lett. **30**(18), 2363–2365 (2005).
3. M. Han, F. W. Guo, and Y. F. Lu, "Optical fiber refractometer based on cladding-mode Bragg grating," Opt. Lett. **35**(3), 399–401 (2010).
4. B. Gauvreau, A. Hassani, M. Fassi Fehri, A. Kabashin, and M. A. Skorobogatiy, "Photonic bandgap fiber-based Surface Plasmon Resonance sensors," Opt. Express **15**(18), 11413–11426 (2007).
5. N. Skivesen, A. Têtu, M. Kristensen, J. Kjems, L. H. Frandsen, and P. I. Borel, "Photonic-crystal waveguide biosensor," Opt. Express **15**(6), 3169–3176 (2007).
6. T. Wei, Y. K. Han, Y. J. Li, H. L. Tsai, and H. Xiao, "Temperature-insensitive miniaturized fiber inline Fabry-Perot interferometer for highly sensitive refractive index measurement," Opt. Express **16**(8), 5764–5769 (2008).
7. Y. J. Rao, M. Deng, D. W. Duan, X. C. Yang, T. Zhu, and G. H. Cheng, "Micro Fabry-Perot interferometers in silica fibers machined by femtosecond laser," Opt. Express **15**(21), 14123–14128 (2007).
8. G. Z. Xiao, A. Adnet, Z. Y. Zhang, F. G. Sun, and C. P. Grover, "Monitoring changes in the refractive index of gases by means of a fiber optic Fabry-Perot interferometer sensor," Sensor. Actuat. A-Phys **118**, 177–182 (2005).
9. B. Qi, G. R. Pickrell, J. C. Xu, P. Zhang, Y. H. Duan, W. Peng, Z. Y. Huang, W. Huo, H. Xiao, R. G. May, and A. Wang, "Novel data processing techniques for dispersive white light interferometer," Opt. Eng. **42**(11), 3165–3171 (2003).
10. J. J. Tian, Q. Zhang, T. Fink, H. Li, W. Peng, and M. Han, "Tuning operating point of extrinsic Fabry-Perot interferometric fiber-optic sensors using microstructured fiber and gas pressure," Opt. Lett. **37**(22), 4672–4674 (2012).
11. R. C. Kamikawachi, I. Abe, A. S. Paterno, H. J. Kalinowski, M. Muller, J. L. Pinto, and J. L. Fabris, "Determination of thermo-optic coefficient in liquids with fiber Bragg grating refractometer," Opt. Commun. **281**(4), 621–625 (2008).
12. http://www.refractometer.pl/refraction-datasheet-ethanol.
13. M. Daimon and A. Masumura, "Measurement of the refractive index of distilled water from the near-infrared region to the ultraviolet region," Appl. Opt. **46**(18), 3811–3820 (2007).

#184892 - $15.00 USD Received 4 Feb 2013; revised 3 Mar 2013; accepted 3 Mar 2013; published 8 Mar 2013

1. Introduction

Fiber-optic refractive index (RI) sensors have received a great deal of attention due to their important applications in biosensing and chemical sensing and their many advantages such as immunity to electromagnetic interference, remote sensing capability, small size and high sensitivity. Many of them are based on the evanescent field interaction with the liquid being measured, such as etched fiber Bragg gratings [1], long period gratings [2, 3], fiber devices based on surface plasmon resonance [4], and photonic crystal waveguides [5]. However, as most of the light energy is contained in the fiber glass material, evanescent-field based sensors suffer from low RI sensitivity, nonlinear RI response, and large temperature cross-sensitivity. These drawbacks can be overcome by a Fabry-Perot (FP) interferometer (FPI)-based RI sensor whose cavity can be filled with the liquid being measured, resulting in a complete overlap between the optical field and the medium being measured. The period of the interferometric fringes of an FPI can be used to obtain the cavity optical length that is linearly proportional to the RI of medium in the cavity. The small thermal expansion coefficient of the silica material renders the sensor's insensitivity to temperature variations. Such a sensor has been fabricated by machining a micro-notch into the core of a single-mode fiber (SMF) to form a fiber in-line FPI using a femtosecond (fs) laser [6]. This sensor shows high RI sensitivity and low temperature cross-sensitivity. However, fs-laser micromachining is a relatively complicate and expensive process. The rough surface from the fs-laser ablation may lead to low fringe visibility and large signal loss due to the light scattering from the surface [7]. The micro-notch in a fiber may greatly compromise the mechanical strength of the sensor. More importantly, the sensor needs to be immersed in the liquid for RI measurement due to the open micro-notch structure, which requires large amount of sample and is not compatible with microfluidic systems.

In this paper, we report a novel fiber in-line FPI sensor with robust structure and microfluidic capability for highly sensitive RI measurement of liquid samples. The microfluidic FPI sensor is based on a fiber hollow tube sandwiched by two cleaved microstructured fibers (MFs). The sensor reported here not only possesses all the advantages of fiber inline FPI sensors, including small size, high RI sensitivity, linear RI response, and low temperature cross-sensitivity, but also overcome many of the drawbacks associated with fs-laser micromachined FPI sensors. The micro-sized holes in the MFs naturally function as microfluidic channels that can be used to efficiently and conveniently deliver the liquid sample into and out of the sensor. Due to the microfluidic capability enabled by the MFs, only sub-microliter sample is required. The fabrication process is low cost and maintains the intact fiber and tube structure of the fabricated sensor. The smooth cleaved fiber end faces lead to high fringe visibility.

2. Sensor structure and fabrication

The structure of the fiber-inline FPI RI sensors is schematically shown in Fig. 1(a). Two spans of MFs are used as the lead-in fiber and the reflection fiber that are spliced with a span of hollow silica tube. The endfaces between the fiber and the tube function as the partial mirrors that form the FP cavity and tube functions as the sample chamber. As shown in Fig. 1(b), the MF (purchased from Fibertronix, Sweden) has a cladding diameter of 125 μm and a germanium-doped core whose diameter is 6 μm. The cladding has two symmetric air holes that run along the whole length of the fiber. The holes have similar diameters of 26 μm and are separated by a center-to-center distance of ~60 μm. The holes of the lead-in MF are opened at a distance to the FP cavity and are connected to a pressure/vacuum pump. As a result, using the air holes of the MF as microfluidic channels, the liquid sample can be conveniently drawn into or pushed out of the FP cavity by applying negative or positive pressure in the holes of the lead-in MF. It is worth noting that the light is guided by the core of the MF and does not penetrate into the micro-sized holes in the cladding, which are merely used as microfluidic channels.

#184892 - $15.00 USD Received 4 Feb 2013; revised 3 Mar 2013; accepted 3 Mar 2013; published 8 Mar 2013

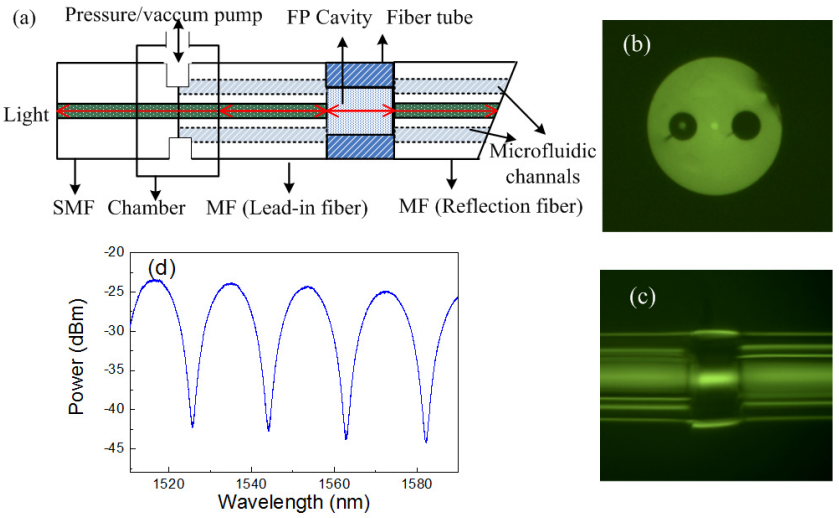

Fig. 1. (a) Structure of the fiber-optic RI sensor; (b) Cross-sectional view of the MF used for the sensor fabrication; (c) Picture of the FPI region of the senor; (d) Interferometric fringes of a fabricated sensor in air.

The specific fabrication process of the sensor is as follows. A ~1.2 m long MF used as the lead-in fiber was spliced with a fused silica fiber hollow tube, which has the same outer diameter as the fiber and an inner diameter of 75 μm, using the manual mode of a fiber splicer. The arc power of splicer was set at a relative low level to ensure that the air holes of MFs did not collapse during the splicing process. Then the fiber tube was cleaved to a specified length facilitated by an optical microscope and a linear translational stage. The cleaved fiber tube was then spliced to another piece of MF to form a FP cavity. Figure 1(c) is a microscope picture of the FP area of the fabricated sensor. In order to remove the undesirable reflection from the far end of the reflection MF, the fiber was terminated with an angle ($> 8°$) by a diamond pencil. The length of the reflection fiber after cutting was approximately 5 mm. The reflection spectrum of the fabricated sensor in air was measured by a fiber sensor interrogator (Micron Optics: sm125) and is shown in Fig. 1(d). The fringe visibility of the sensor is more than 20 dB, which is much larger than the 5 dB fringe visibility (in air) of the inline FPI sensor fabricated by fs-laser micromachining [6]. For a low finesse FP device, the optical length of the cavity can be calculated from the interferometric fringes by [8, 9]:

$$L \cdot n = \frac{1}{2}\left(\frac{\lambda_{v1}\lambda_{v2}}{\lambda_{v2} - \lambda_{v1}}\right), \tag{1}$$

where λ_{v1} and λ_{v2} are the center wavelengths of two adjacent valleys of the interferometric fringes and n is the RI of the medium in the cavity. Assuming the RI of air is 1.0003 and from Fig. 1(d), the FP cavity length is estimated to be 64.12 μm. With an inner diameter of 75 μm of the silica tube, the volume of the cavity, which can be used to approximate the minimum amount of liquid sample required by the sensor, is calculated to be 0.28 μL.

To apply controlled gas pressure in the sensor cavity through the holes of the lead-in MF, the holes need to be opened and connected to a pressure/vacuum pump system. This was achieved by etching the MF at the MF/SMF splicing junction using hydrofluoric acid (HF). The etching process, which was detailed in [10], was carried out before the fabrication of fiber-optic sensor. After the air holes were opened by HF etching, the etched region of the fiber was placed inside a chamber that was connected to a gas pressure/vacuum pump (Additel: ADT919) to apply positive or negative pressure in the holes.

#184892 - $15.00 USD Received 4 Feb 2013; revised 3 Mar 2013; accepted 3 Mar 2013; published 8 Mar 2013

3. Experiment and discussion

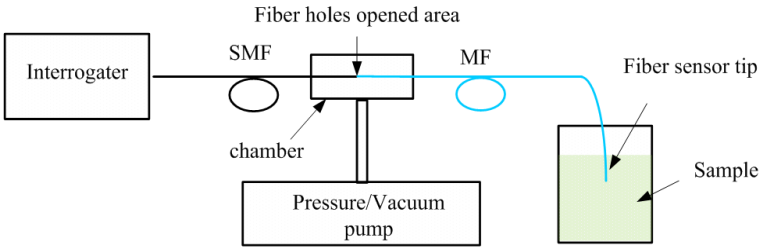

Fig. 2. Schematic of the experimental setup for RI measurement of liquid.

We measured the RI of deionized (DI) water and ethanol using the set up schematically shown in Fig. 2. The reflection spectrum of the sensor in air was first recorded by the sensor interrogator (Micron Optics: sm125). Then the tip of the reflection MF was immersed in the liquid sample and subsequently a negative pressure was applied by the pump to draw the liquid into the sensor through the microfluidic channels in the reflection MF. As the liquid filled the FP cavity, the reflection spectrum was recorded by the sensor interrogator again. After the measurement, the tip of the reflection MF was removed from the liquid sample and positive pressure was applied to push the liquid in the cavity out of the sensor through the microfluidic channels. We have found that the spectrum of the sensor always recovered back to that in the air, suggesting a complete removal of the sample in the cavity that did not influence the next liquid RI measurement. By this way, therefore, it can achieve a reliable, repeatable, and high-sensitivity liquid IR measurement. It is noted that due to the low viscosity compared with water, ethanol was much easier to be drawn into and pushed out of the sensor cavity. Figure 3 shows the reflection spectra when the sensor cavity was filled with air, DI water, and ethanol. Again, assuming the RI of air is 1.0003, the physical length of the FP cavity, L, can be calculated from Eq. (1) from the fringes of the sensor in air. With L known and using Eq. (1) again, the absolute RIs of DI water and ethanol are calculated to be 1.3514 and 1.3639, respectively, from their respective interferomertic fringes. We note that the calculated absolute RIs are larger than previously reported values at the optical wavelength of 1550 nm and similar temperature (1.323 for water and 1.354 for ethanol at 21 °C) [11]. This discrepancy needs to be further investigated.

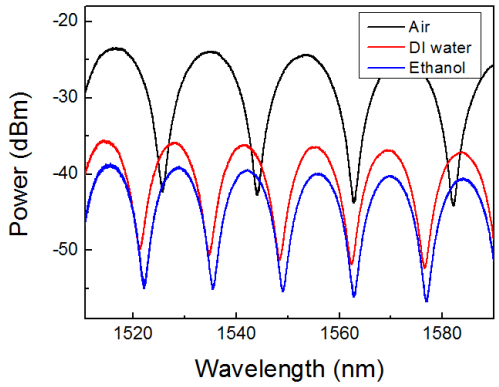

Fig. 3. Reflection spectra when the sensor FP cavity was filled with air, ID water, and ethanol.

Although Eq. (1) can obtain the absolute RI of a sample, it is sensitive to measurement errors in the fringe period and offers inadequate resolution in many applications. In cases where only the relative RI changes are of interest, relative RI measurement can be achieved

#184892 - $15.00 USD Received 4 Feb 2013; revised 3 Mar 2013; accepted 3 Mar 2013; published 8 Mar 2013

with much higher resolution by tracing the spectral shift of a specific point of the fringe (e.g. one fringe peak or valley). The spectral shift, $\Delta\lambda$, caused by a RI change, Δn, is given by [6]

$$\Delta n = \frac{\Delta\lambda}{\lambda} n, \tag{2}$$

where λ and n are, respectively, the wavelength of the fringe point and the absolute RI of the sample. Using this method, we measured the RI changes caused by small changes in the concentration of ethanol solution in DI water. The weight concentration of the ethanol solution was increased from 0 to 11.11% with a step size of 1.2% by sequentially adding 1.25 ml pure ethanol in 80 ml DI water, resulting in a total RI change of approximately 0.008 RIU (RI unit). For each step, the measure procedure was similar to that used in obtaining Fig. 3. Again, it is noted that, for each step and before next measurement, the liquid was completely pushed out of the sensor through the microfluidic channels by the positive pressure applied in the lead-in MF and the interferogram recovered to that in air. The measured reflection spectra when the sensor cavity was filled with the ethanol solution of different concentrations are shown in Fig. 4(a). It is seen that, as the ethanol solution concentration increased, the fringes of the sensor shifted to the longer wavelength. Specifically, the wavelength position of the fringe valley at 1548.38 nm in the DI water shifted to 1556.91 nm for the 0.008 RIU change, corresponding to a RI sensitivity of 1051 nm/ RIU, which is comparable to that reported in [6]. The wavelength position of a fringe valley was found through a second-order polynomial fitting to the measured spectrum around the fringe valley. Using the wavelength position of the same fringe valley, the RI changes are calculated from Eq. (2) and the results are shown in Fig. 4(b), which agree well with the results in [12] [also shown in Fig. 4(b)].

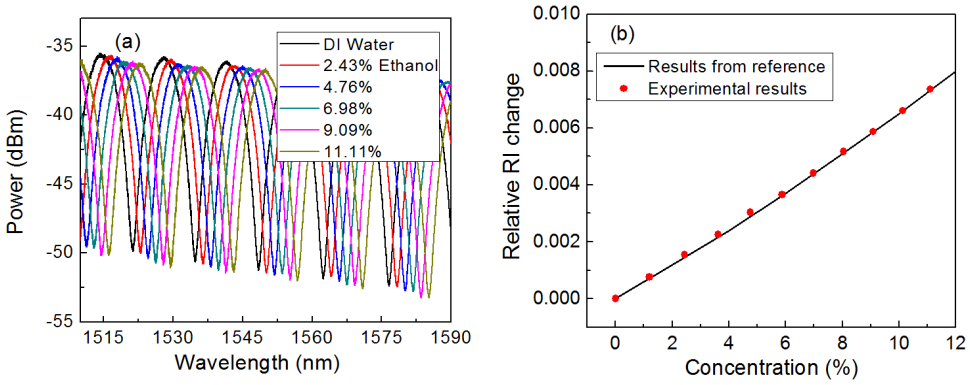

Fig. 4. (a) Reflection spectra of the RI sensor when the FP cavity was filled with ethanol solutions of different concentrations; (b) Calculated RI change as a function of the ethanol concentration and comparison with results in [12].

As discussed earlier, the RI sensor with its inherent microfluidic channel and microfluidic pumping system can provide convenient, repeatable, and reliable RI measurement using a small amount of sample. To further verify the repeatability of the sensor, we repeated the RI measurement of DI water several times in a prolonged time of more than 3 days. The same procedure described above was followed and the same DI water sample was used for each measurement. The measured spectra and the relative RI change calculated from Eq. (2) are shown in Fig. 5(a) and 5(b), respectively [the detailed spectra around the fringe valley for the relative RI calculation are shown in the inset to Fig. 5(b)].The peak-to-peak variation of the calculated RIs is only 1×10^{-5}. Noting that water has a thermo-optic coefficient (dn/dT) of $\sim -8 \times 10^{-5}$/°C [13], a significant contribution to the observed RI variations may be from the temperature changes of the ambient environment.

#184892 - $15.00 USD Received 4 Feb 2013; revised 3 Mar 2013; accepted 3 Mar 2013; published 8 Mar 2013

Another advantage of the FPI sensor is the low temperature cross-sensitivity due to the small thermal-expansion coefficient of the silica material of the tube (5.5×10^{-7}/ °C). As the sensor fabrication involves the fusion splicing of the MFs and the silica tube, residual thermal stress may be induced in the process. Before measurement of the temperature response, the sensor was annealed in a furnace by gradually increasing the temperature from room temperature to ~100 °C. Then the reflection spectra of the sensor in air at different temperatures ranging from 22 °C to 105 °C were recorded, as shown in Fig. 6(a). The equivalent RI changes from the temperature variations were then calculated from Eq. (2) using a fringe valley and the results are shown in Fig. 6(b) [the inset to Fig. 6(b) shows the spectra around the fringe valley]. It is seen that the variation of the equivalent RI was less than 3×10^{-5} for the temperature change of more than 80 °C, showing excellent temperature stability of the sensor. It is worth noting that the calculated equivalent RI shows an overall trend of deceasing as the temperature increases, indicating that the FP cavity length change from the relaxation of the residual thermal stress may be more dominant than that from the thermal expansion of the silica tube.

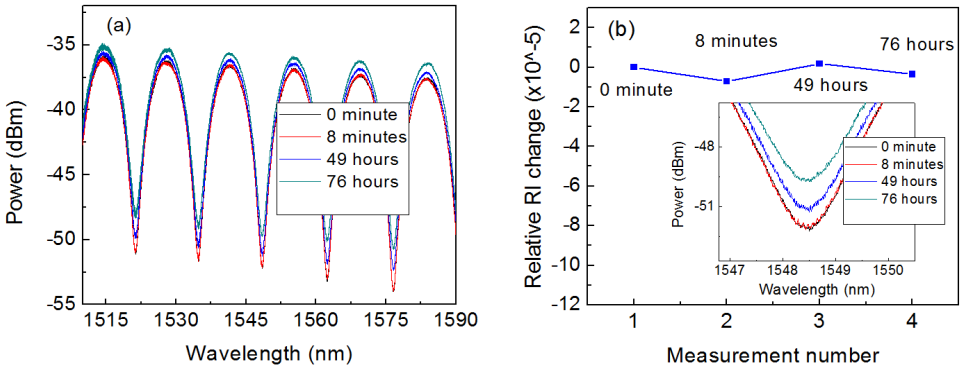

Fig. 5. Sensor repeatability test. (a) Reflection spectra of the sensor for several measurements of DI waters; (b) Calculated RI changes; inset: enlarged view of the spectra around a fringe valley.

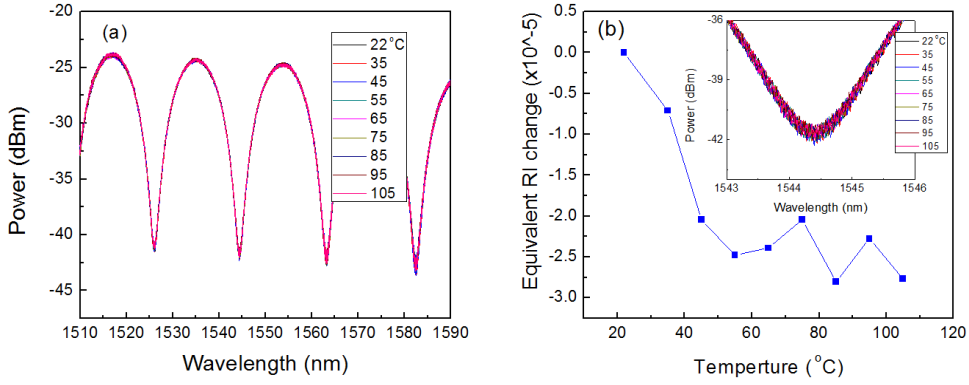

Fig. 6. Test of the sensor's temperature cross-sensitivity. (a) Reflection spectra of the sensor at different temperatures in air; (b) Calculated equivalent RI changes; inset: enlarged view of the spectra around a fringe valley.

#184892 - $15.00 USD Received 4 Feb 2013; revised 3 Mar 2013; accepted 3 Mar 2013; published 8 Mar 2013

4. Conclusion

A novel microfluidic RI sensor based on an in-line FPI fabricated with MFs was proposed, fabricated, and studied. The sensor can be fabricated with low cost, possesses a robust, all-silica structure, and has microfluidic capability. Using the micro-sized holes in the MFs as microfluidic channels and a pressure/vacuum pump, the liquid sample can be conveniently and efficiently delivered into and out of the sensor with only sub-μL sample required. The RI sensitivity of the sensor was characterized to be 1051 nm/RIU at the wavelength of 1550 nm. We also have experimentally demonstrated that the sensor has additional advantages of good repeatability and low temperature cross-sensitivity. These advantages make this fiber-optic RI sensor attractive in many applications including chemical and biological sensing.

Acknowledgment

This work was supported by the National Science Foundation under grant EPS-1004094 and the Office of Naval Research under grant N000141110705.

#184892 - $15.00 USD Received 4 Feb 2013; revised 3 Mar 2013; accepted 3 Mar 2013; published 8 Mar 2013